Characterization of sol-gel-derived nano-particles separated from oil sands fine tailings

Majid, Abdul; Argue, Steven; Boyko, V.; Pleizier, G.; L'Ecuyer, P.; Tunney, Jim; Lang, Stephen

Publisher's version / Version de l'éditeur:
https://doi.org/10.1016/S0927-7757(03)00266-8
Colloids and Surfaces A: Physicochemical and Engineering Aspects, 224, August, pp. 33-44, 2003

NRC Publications Record / Notice d'Archives des publications de CNRC:
https://nrc-publications.canada.ca/eng/view/object/?id=a026f2d4-7920-4f2e-8239-2fa78a50e774
https://publications-cnrc.canada.ca/fra/voir/objet/?id=a026f2d4-7920-4f2e-8239-2fa78a50e774

ELSEVIER

Colloids and Surfaces A: Physicochem. Eng. Aspects 224 (2003) 33–44

COLLOIDS AND SURFACES A

www.elsevier.com/locate/colsurfa

Characterization of sol–gel-derived nano-particles separated from oil sands fine tailings☆

A. Majid [a,*], S. Argue [a], V. Boyko [a], G. Pleizier [a], P. L'Ecuyer [a], J. Tunney [a], S. Lang [b]

[a] *Institute for Chemical Process and Environmental Technology, National Research Council of Canada, Ottawa, Ont., Canada K1A 0R9*
[b] *Steacie Institute for Molecular Sciences, National Research Council of Canada, Ottawa, Ont., Canada K1A 0R9*

Received 11 June 2002; accepted 30 December 2002

Abstract

Methodology has been developed to separate nano-particles of amorphous material from Syncrude fine tailings. Both, separated finer solids and residual coarser solids, were characterized by elemental analysis, X-ray powder diffraction, XPS, SEM, infrared spectroscopy, solid-state NMR, density, and surface area measurements. Based on the results of infrared and X-ray diffraction, the amorphous minerals identified in finer solids included allophanes, halloysite, ferrihydrite, and amorphous silica. The finer fraction also contained some crystalline material consisting of muscovite and traces of quartz. The residual coarser solids consisted mostly of quartz, muscovite, and kaolinite.

Keywords: Allophanes; Amorphous solids; Characterization; Clays; Fine tailings; Oil sands; Nano-particles

1. Introduction

The extraction of bitumen from Athabasca oil sands, using the hot water extraction process, results in the accumulation of large volumes of fluid wastes called fine tailings [1,2]. A general description of fine tailings would be a complex system of clays, minerals, and organics. According to Camp [3], fine tailings show little tendency to dewater, even when subjected to mechanical dewatering procedures. These clay tailings are acutely toxic to aquatic organisms, and are currently being stored in large tailings ponds. The buildup of these partially settled clay tailings presents not only an environment problem but also a significant repository for non-recyclable water, which eventually must be reclaimed.

The reason for the intractability of the clay tailings has been a subject of several studies [4–7]. Based on the results of published work, it is generally believed that a combination of residual organics and fine clay particles contribute to the stability of fine tailings. Yong and Sethi [2] have attributed the high water-holding capacity of fine

☆ Issued as NRCC No. 46441

* Corresponding author. Tel.: +1-613-993-2017; fax: +1-613-991-2384.
E-mail address: abdul.majid@nrc.ca (A. Majid).

0927-7757/03/$ - see front matter © 2003 Published by Elsevier B.V.
doi:10.1016/S0927-7757(03)00266-8

tailings to the presence of amorphous minerals such as iron oxide and clays.

Our group at NRC has been actively involved in research dealing with various aspects of fine tailings [5–14]. As a result, we have developed a number of fractionation schemes to separate fine tailings into various components. The objective of this work was twofold. First to develop fractionation schemes for the separation of amorphous solids (ASs) from oil sands fine tailings, and secondly to characterize the separated solids by both physical and chemical methods. In our previous communications, we have reported preliminary data on the separation and characterization of ASs from oil sands fine tailings using the Tiron extraction method [5,15,16]. In this investigation, we have separated ASs of different composition from Syncrude fine tailings using a combination of sol–gel chemistry and a number of separation techniques developed in-house. The solid fractions have been characterized by elemental analysis, X-ray diffraction (XRD), XPS, SEM, infrared spectroscopy, solid-state nuclear magnetic resonance (NMR), and surface area measurement. The characteristics of the ASs obtained by different separation techniques have been compared.

2. Materials and methods

2.1. Materials

Aqueous tailings samples, used in this investigation, were obtained from the 17 m level of the Syncrude tailings pond. The physicochemical properties and handling procedures for these samples have been reported previously [7].

Tiron (4,5-dihydroxy-1,3-benzene-disulphonic acid disodium salt) was obtained from Sigma Chemicals, Inc. It was used as 0.1 M aqueous solution containing 5.3 g of anhydrous sodium carbonate. The final pH of the solution was adjusted to 10.5 with sodium hydroxide. The solution was kept in a polypropylene bottle and stored in a refrigerator for a maximum of 1 month. The solution pH dropped during storage and was adjusted to 10.5 before use.

All other reagents were obtained from Aldrich and used as received.

2.2. Removal of residual bitumen and hydrophobic solids

A sample of fine tailings (500 g) was gently agitated with stainless steel balls in a rotating polyethylene bottle [7]. Residual bitumen and hydrophobic solids were collected as a surface coating on the balls. The balls containing bitumen and hydrophobic solids were separated from clean tailings using a 150-μm stainless steel screen.

2.3. Extraction and/or dispersion of amorphous solids

The clean tailings were divided into two portions for treatment to separate ASs. One portion was centrifuged at $1000 \times g$ for 2 h to separate coarser solids from the suspension containing finer solids. The second portion was mixed with one of the reagents used for the dissolution and/or dispersion of ASs, and the contents agitated. The reagents included Tiron, sodium hydroxide, and sodium silicate. The contents were agitated in an end-over-end fashion for 72 h at 30 ± 2 rpm. The contents from this treatment were centrifuged at $500 \times g$ for 10 min to separate suspension/solution containing ASs from coarser solids. Suspensions/solutions from both treatments were used for the separation of ASs.

2.4. Separation of amorphous solids

The separation of the ASs from suspension/solution fractions was carried out by precipitation with a mineral acid (HCl). A typical treatment involved acidification of the suspension/solution to $pH \cong 1$, when ASs precipitated as a gel, releasing free water. The contents were centrifuged and the wet sediment washed several times with distilled water followed by isopropanol. Finally, the wet cake containing ASs was dried at 80 °C under vacuum. A sample of amorphous silica was prepared for comparison using a published procedure [17].

2.5. Measurements

^{29}Si NMR spectra were recorded at 40 MHz on a TecMag Apollo series spectrometer. Samples were spun at 4.5 kHz in zirconia rotors in a Doty 7 mm MASS probe. The 90° pulse length was 10 μs. A 10-s delay between pulses was found to be adequate, and spectra were accumulated overnight. ^{27}Al NMR spectra were recorded at 78 MHz on a Bruker AMX-300 spectrometer, using a Doty 5 mm mass probe, a 5-mm zirconia rotor, and 8–8.5 kHz MASS. A pulse length of 1 μs was used, and 1000 scans were acquired, with a 0.5-s delay between scans. A noticeable probe background was subtracted. The chemical shifts of aluminium and silicon were referenced against external 1 M aqueous aluminium nitrate and neat tetramethyl silane (TMS), respectively.

PAS-FTIR (photo-acoustic Fourier transform infrared spectroscopy) spectra were collected using an MTEC Model 300 photo-acoustic detector combined to a Bruker IFS 66/S FTIR spectrometer. 500 scans were collected at a resolution of 8 cm^{-1} in the rapid scan mode. 64 scans of carbon black were used as reference, and helium was the purge gas.

XPS was performed with a physical electronics (Perkin–Elmer, Eden Prairie, MN) model 550 instrument. Monochromatic Al Kα radiation was used. The dry samples were pressed into indium foil for analysis. Survey spectra were collected using pass energies of 188 eV, while high-resolution spectra were recorded with a 22-eV pass energy. An electron flood gun was used to neutralize the charge during the experiment. Binding energies (BEs) were referenced to the carbon–carbon bond, which was assigned a BE of 285 eV. Atomic compositions were estimated using a standard program provided with the instrument. During analysis, the pressure inside the instrument was always below 5×10^{-9} Torr (< 0.7 μPa).

Scanning electron micrographs were recorded using a JEOL model JSM-5300 instrument operated at 10 kV. The samples were coated with a thin carbon layer to impart conductivity.

Specific surface areas, pore volumes, and pore size distributions were determined using a Micromeritics Gemini III 2375 apparatus. The density of the materials was determined by a Pycnometry measurement with helium using Micromeritics Accupyc 1330 apparatus. Inorganic elemental analysis was carried out using inductively coupled plasma atomic emission spectrometry (ICP-AES).

Cation exchange capacity (CEC) was measured using the $BaCl_2$ method [18].

X-ray powder diffraction data were collected between $2\theta = 5$–$100°$ with a scan rate of $2° \text{ min}^{-1}$ at room temperature on a Scintag XDS 2000 with a theta–theta geometry and a copper X-ray tube. The diffractometer had a pyrolytic graphite monochromator in front of the detector. The samples were mounted on a zero background sample holder made of an oriented silicon wafer.

Particle size analyses were carried out using a Malvern zetasizer.

3. Results and discussion

3.1. Physicochemical characterization

Yong and Sethi [2] have attributed the stability of fine tailings to the presence of amorphous materials such as iron oxides and disordered clays. However, their proposed structure of fine tailings did not get much support because of the lack of progress in the detection and separation of amorphous minerals from fine tailings. Many difficulties arise in the characterization of inorganic amorphous materials. By their very nature, amorphous substances are difficult to detect and estimate, and frequently their presence is determined by implication rather than by direct measurement.

We have now successfully separated the so-called ASs from Syncrude sludge pond tailings using a number of selective dissolution methods. These treatments are known to remove substantial amounts of the finely divided ASs such as allophanes, aluminosilicates, and oxides of iron, aluminum, and silicon [16]. These selective chemical dissolution methods depend on the high specific surface area and lower thermodynamic stability of poorly ordered materials, which results in a higher dissolution rate than for crystalline minerals [19]. The physicochemical characteristics

of finer solids recovered using chemical dissolution techniques and the residual extracted solids were compared with the blank solids as well as the solids obtained by dispersion with sodium silicate.

Table 1 lists description and some characteristics of all the samples studied in this investigation. Two of the treatments (NaOH and Tiron) resulted in the dissolution of the fine mineral particles with associated humic matter giving a dark black solution. Centrifugation and dispersion by Na_2SiO_3 gave suspensions of fine solids. The results show that the highest amount of solids was extracted by NaOH. The amount of solids extracted by NaOH was almost equal to the amount of solids dispersed by sodium silicate. The least amount of the finer solids was extracted by Tiron.

All samples had considerable quantities of adsorbed insoluble organic matter as indicated from the loss on ignition values shown in Table 1. The high levels of organic matter content indicate that there is a very important interaction between the organic and inorganic materials in these solids. This organic matter is mostly humic and may be acting as a glue between mineral particles resulting in aggregate formation [7,9,13,20–22]. The samples were ashed using a low-temperature ashing technique [23].

The measured density of the ashed finer solids (2.61 ± 0.02 g cm^{-3}) varied very little for solids separated by different schemes. The density value for finer solids was also comparable to the density of allophanes, halloysites, imogolite, and kaolin minerals [24]. The density of coarser residual solids was slightly higher than the value for finer solids (2.71 ± 0.1 g cm^{-3}).

Specific surface area of the solids was determined after ashing to remove adsorbed organic matter. The nitrogen adsorption isotherms at 77 K for the calcined samples represented a type IV isotherm in the IUPAC classification [25]. Characteristic features of the type IV isotherm are its hysteresis loop, which is associated with capillary condensation taking place in mesopores, and the limiting uptake over a range of high p/p^0. Compared with extracted residual solids (coarser solids), all finer solids obtained by the sol–gel processing of the extracts and suspensions had high surface areas. The solids obtained from washing of the recovered bitumen had the highest surface area. The specific surface area values of the finer solids approach the values reported for heated silica–alumina gels [26]. Surface area and pore size determine the accessibility to active sites and this is often related to catalytic activity and selectivity in catalyzed reactions. The relatively low cost and microporosity of the ASs separated from fine tailings render these materials excellent candidates for potential applications in heterogeneous catalysis [27].

CEC values of the finer solids range from 14 to 37 Cmol[+] kg^{-1}. These values are higher than those reported for kaolinite minerals but within the range for halloysites, allophanes, and illites [28]. The values for extracted coarser solids fall within the range reported for kaolinite and muscovite minerals.

Elemental content of these solids suggests that compared with extracted residual coarser fraction, finer solids obtained by the sol–gel processing of the extracts and suspensions may be enriched with clay minerals as indicated from their Si and Al contents which fall in the range of clay minerals [29]. The presence of greater amounts of silica minerals, such as quartz in the extracted coarser solids fraction, accounts for higher levels of silica in these solids.

The distribution of iron in these solids was of particular interest because of its potential role in the stability of fine tailings [2]. In general, the finer solid fractions had greater iron content compared with coarser solids. The least amount of iron was found in the NaOH-extracted solids.

Fig. 1 demonstrates the effect of iron content on the specific surface area of both fine as well as coarser solids. At higher iron content, the specific surface area is decreased for both finer as well as the coarser solids; the effect being more pronounced for the latter. The effect is also more pronounced for samples containing higher iron content. The data for the finer solids obtained from the washing of bitumen do not appear to correlate with the data for other samples. The fact that the surface area increases with decrease in iron content suggests the agglomeration of finer particles by iron oxides thus supporting the theory

Table 1
Sample description and physicochemical characteristics of solids separated from bitumen-free clean tailings

Test No.	Sample No.	Description	Yield[a]	LOI[b]	Density[c]	Surface area[d]	CEC[e]	Elemental analyses (wt.%/wt.%)							SiO_2 :Al_2O_3
								Si	Al	Fe	Ca	Na	K	Mg	
1	F1	Washings from recovered bitumen	–	16.1	2.62	129	17.8	24	16	3.0	0.33	0.25	2.9	1.0	1.7
1	F2	Centrifuged suspension	9.8 ±0.6	14.4 ±1.3	2.57	107 ±23	17.1 ±0.7	23	15	2.7	0.03	0.53	2.8	0.9	1.7
1	C1	Centrifuged sediment	89.5 ±0.4[f]	7.4 ±1.7	2.69	23	7.7	33	16	2.1	0.6	2.1	3.8	1.3	2.3
3	F3	Na_2SiO_3 dispersed solids	5.3 ±0.3	17.5 ±0.7	2.58	107	14.3	28	17	2.1	2.7	0.93	3.1	1.1	1.9
4	F4	Tiron extract	3.7 ±0.2	21.8 ±3.8	2.60	105±19	17.8 ±1.3	26.3 ±1.2	16.3 ±0.5	3.3 ±0.8	0.37 ±0.19	0.8 ±0.5	2.4 ±0.6	0.72 ±0.3	1.8
4	C2	Tiron-extracted clean solids	96.3 ±0.2[f]	4.1 ±0.2	2.78	12.8	7.4	31	13	2.5	0.04	0.54	3.0	4.2	2.7
5	F5	NaOH extract	5.1 ±0.2	23.7 ±0.6	2.61	93	21.2	25	16	3.9	0.24	0.79	2.8	1.8	1.8
5	C3	NaOH-extracted clean solids	94.9 ±0.2[f]	4.9 ±0.2	2.71	31	ND	28	12	1.5	0.18	0.43	2.0	2.5	2.7

ND, not determined.
[a] wt.%/wt.% of total solids
[b] Loss on ignition at 450 °C
[c] In g cm^{-3}
[d] In m^2 g^{-1}
[e] Cmol[+] kg^{-1}
[f] By difference.

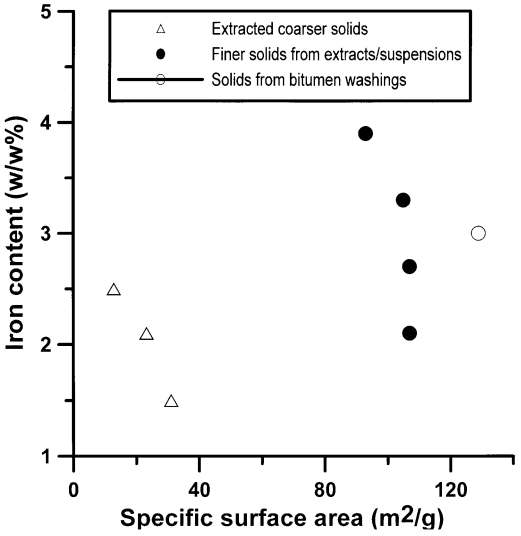

Fig. 1. The effect of iron content on the specific surface area of solids.

of the cementation of clay particles by amorphous oxides [2,29].

Magnesium and potassium are significant components of both finer as well as coarser solids. The distribution of potassium is essentially similar in the finer and coarser fractions, but magnesium appears to be enriched in the Tiron and NaOH extracts.

The silica to alumina ratios for finer solids varied from 1.7 to 1.9. This value was considerably lower than the value for coarser solids, which ranged from 2.3 to 2.7. The values of silica to alumina ratio for finer solids is in the same range as reported for kaolinite and allophanes [30,31]. The presence of silica minerals of quartz and muscovite in coarser fraction accounts for the higher silica to alumina ratio values for these solids.

3.2. Particle size distribution

Table 2 lists the particle size distribution in the finer solids. More than 50% of all samples contained particles less than 100 nm in size. Tiron and NaOH extracts contained the maximum amount of smaller size particles. The biggest size particles were found in fractions F3 and F5. These particles ranged in size from 200 to 600 nm. The biggest size particles found in fractions F1, F2, and F4 were around 200 nm.

3.3. X-ray diffraction

The XRD analyses were performed on all samples and are shown in Fig. 2. All finer fractions had essentially similar patterns differing only in the relative intensity of various peaks. A typical XRD pattern for finer fractions is shown in Fig. 2(a). The XRD pattern for the coarser cleaner solids obtained after the removal of finer material is represented in Fig. 2(b).

The amorphous nature of the finer solids is evident from the considerable broadness of the peaks. Also, the good resolution with sharper peaks in XRD pattern of the coarser solids suggests very little amorphous material remaining with the coarser solids implying effective separation of the material from the crystalline minerals.

Many difficulties arise in the characterization of amorphous materials. By their very nature, amorphous substances are difficult to detect and estimate, and frequently their presence is determined by implication rather than by direct measurement. Further complications arise because of the fact that these materials consist of a mixture of several components present in different proportions. Tentative assignments were made based on the comparison with XRD patterns of the standards published in the literature [31–34]. The minerals thus identified are listed in Table 3.

Major minerals in the finer fractions were identified as muscovite and halloysite from characteristic reflections at 1.94, 2.54, 3.29, 4.93, 9.93, and 4.4 and 9.93 Å, respectively [31]. Broad peaks at 3.40 and 2.25 Å suggest the presence of allophane in most of the samples. The presence of allophane-type material is also supported from the fact that these samples contained significant amounts of adsorbed humic matter. Since allophanes are known to be strong adsorbents for humified materials, the exceptionally high levels of organic matter are common to soils of high-allophane content [35].

The presence of kaolinite was suggested in the NaOH extract (peaks at 3.53 and 6.9 Å) [35]. The

Table 2
Particle size distribution in finer solids

Fraction	Description	Particle size distribution (vol.%)		
		20–50 nm	50–100 nm	>100 nm
F1	Washings from recovered bitumen	65	–	35
F2	Centrifuged suspension	3	63	34
F3	Na_2SiO_3 dispersed solids	25	28	47
F4	Tiron extract	36	53	11
F5	NaOH extract	63	24	13

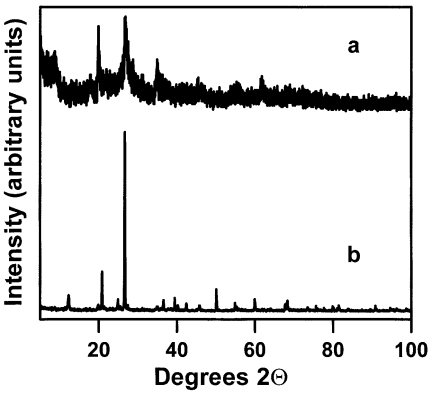

Fig. 2. A typical XRD pattern for (a) finer solids (samples F1–F5); (b) coarser solids (samples C1–C3).

Table 3
Minerals identified from XRD data

Sample	Minerals
F1, F2, F3, F4	Major: muscovite, halloysite
	Minor: allophane, ferrihydrite, amorphous MnO_2, histingite, amorphous silica
C1, C2, C3	Major: quartz, kaolinite
	Minor: muscovite, gibbsite, geothite, feldspar

coarser solids consisted mostly of quartz, kaolinite, and muscovite with minor amounts of other minerals.

3.4. Nuclear magnetic resonance

Solid-state magic angle spinning (MAS), NMR can provide valuable information in the identification of minerals. Fig. 3 shows the ^{29}Si MAS NMR spectra of ultrafine solid samples listed in Table 1. Except sample F5, all the samples show a broad resonance at ~ -98 ppm (Fig. 3(a)) which indicates disordered environment and is characteristic of synthetic aluminosilicate gels and allophanes [5,19]. Feldspars also fall in this region [36]. Sample F5 had a shoulder at ~ -114 ppm in addition to the major peak around -95 ppm (Fig. 3(b)). This resonance may be assigned to Q^4 (0Al) of layered silicates [36].

Fig. 4 shows a typical ^{27}Al MAS NMR spectrum of ultrafine solids. The detectable Al atoms show, in addition to a peak for octahedral Al at about 0 ppm, another ill-defined weak peak for tetrahedral Al at about 65 ppm [4]. A similar spectrum has been reported for synthetic amorphous aluminosilicate gel [37].

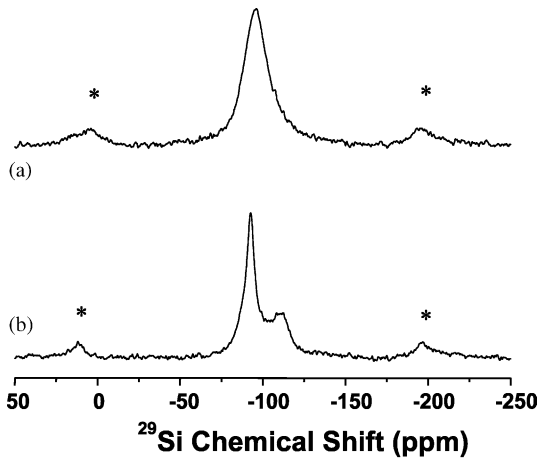

Fig. 3. ^{29}Si MAS NMR spectra of ultrafine solids: (a) samples F1–F4 and (b) sample F5.

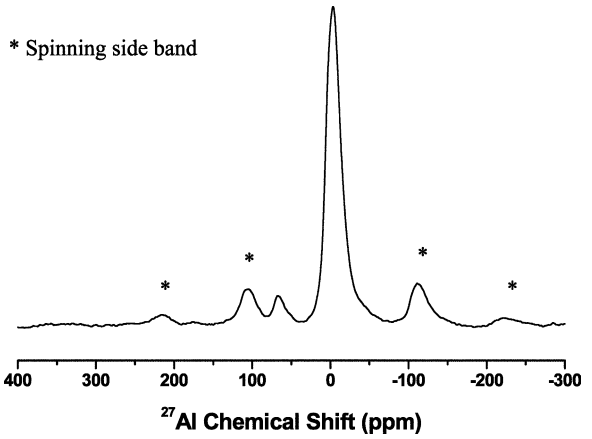

Fig. 4. A typical ^{27}Al MAS NMR spectrum for ultrafine solids.

3.5. Infrared spectra

The technique of infrared absorption has previously been applied with some success to colloidal clays [38–40] and may be a useful tool for the identification of amorphous colloids separated from Syncrude fine tailings. However, the identification of the infrared bands in clay minerals remains very difficult because of their complicated and non-constant composition. The weak intensities which are commonly found in this category of minerals and which are caused by substitutions and poor ordering form another obstacle. The principal forms of amorphous inorganic materials, which occur in soils are the oxides, or more usually, the hydrous oxides of iron, aluminum, manganese, or silicon, either separately or combined. XRD data for ASs separated from fine tailings suggest the presence of allophanes, amorphous silica, and halloysites as amorphous components and muscovite as major crystalline impurity. Identification of these minerals present as a mixture is difficult from infrared spectrum because of other overlapping absorptions. Further complications arise from the fact that the characteristic absorption bands for the poorly crystalline samples are not clearly distinguishable. The interpretation of absorption spectra of ASs separated from Syncrude fine tailings, therefore, must be made with caution. The assignment of the various bands in the infrared spectra is based on the published work for clays and related minerals [19,41–45].

Fig. 5(a) shows a typical PAS-FTIR spectrum for finer solids. The spectrum shows dominance of amorphous silicon oxide and/or aluminosilicates such as allophanes as suggested from a broad absorption in the OH region centered around 3300 cm^{-1}. This is further supported from a strong and broad absorption in the Si–O region (900–1100 cm^{-1}). Absorption in the 3600–3700 cm^{-1} region resembles more with the halloysite than kaolinite [19]. A very weak doublet at 780 and 800 cm^{-1} suggests the presence of quartz impurity.

Fig. 5(b) shows a typical PAS-FTIR spectrum for extracted coarser solids. This spectrum contains clearly distinguishable sharp bands that are characteristic of crystalline materials. The spectrum is dominated by the bands of kaolinite at 3700, 3668, 3650, 3615, 1104, 1034, 1010, 940, 920, 700, and 650 cm^{-1}. A doublet at 780 and 800 cm^{-1} is characteristic of the presence of quartz [46]. The absorption in the OH region, centered on about 3300 cm^{-1}, assigned to amorphous material is considerably weaker than in the finer solids. This suggests that a small amount of amorphous material remains unextracted. The sample contains significant amounts of oxidized humic matter as indicated from bands in the 2900 and 1700–2000 cm^{-1} region [43].

3.6. X-ray photoelectron spectroscopy

X-ray photoelectron spectroscopy (XPS) is a widely used analytical technique for investigating the chemical composition of solid surfaces. It is restricted to the top 10 nm of the sample surface. It gives quantitative information on all the elements on the surface (except H and He). XPS results for the finer solids are listed in Table 4. Fig. 6 shows a correlation between the loss on ignition of the finer solids, which is a measure of total organic matter content of the solids, and the amount of carbon on the surface. The data were fitted to a first-order equation with a correlation coefficient of 0.96. The fact that such a correlation exists suggests uniform distribution of organic matter in the bulk and surface. As shown in Fig. 7, a similar correlation was found for iron.

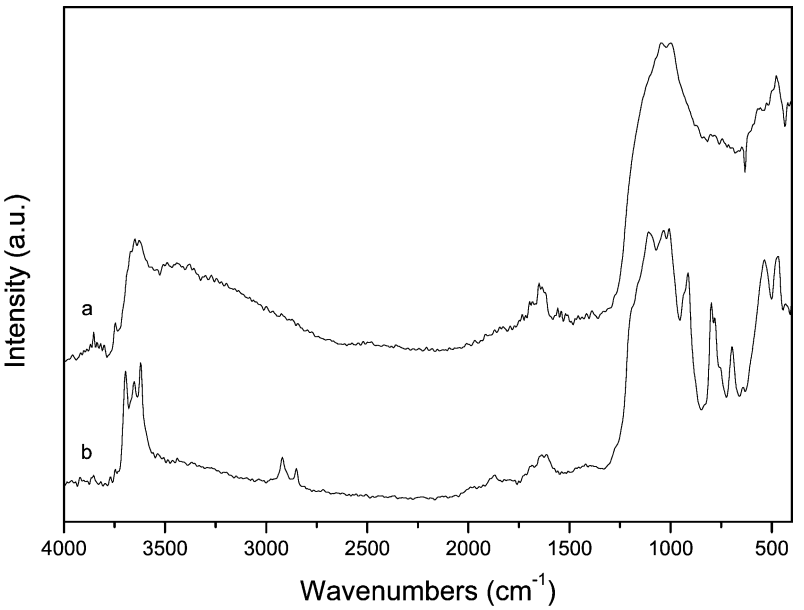

Fig. 5. PAS-FTIR spectra: (a) a typical spectrum for finer solids and (b) a typical spectrum for extracted coarser solids.

Table 4
Atomic concentrations of various elements from XPS

Element	Concentration (at.%)				
	F1	F2	F3	F4	F5
C	10.7	11.1	14.7	24.1	16.7
O	57	56.3	56.3	45.3	55.9
Si	17.6	17.4	15.6	16.5	14.1
Al	12.2	12.6	11.4	12.5	10.9
Mg	0.3	0.4	0.3	0.1	0.3
K	1.4	1.4	1.2	0.9	1.1
Fe	0.8	0.7	0.6	0.8	1.0

Calculated directly based on atomic composition.

Compared with the bulk analyses, the composition of aluminosilicates at the surface of the finer solids was more uniform as indicated from the value of Si:Al ratio (1.36 ± 0.05). This supports the theory regarding a coating of amorphous material on the surface of a mixture of inorganic minerals. The Si 2s and O 1s BEs of this material are similar to those for silica, but distinctly different from those for the sheet silicate kaolinite [47].

The Fe 2p spectral lines at BEs 712 ± 1 and 725 ± 1 eV are consistent with values for Fe^{3+} in geothite, limonite, and hydrous ferric oxides [47].

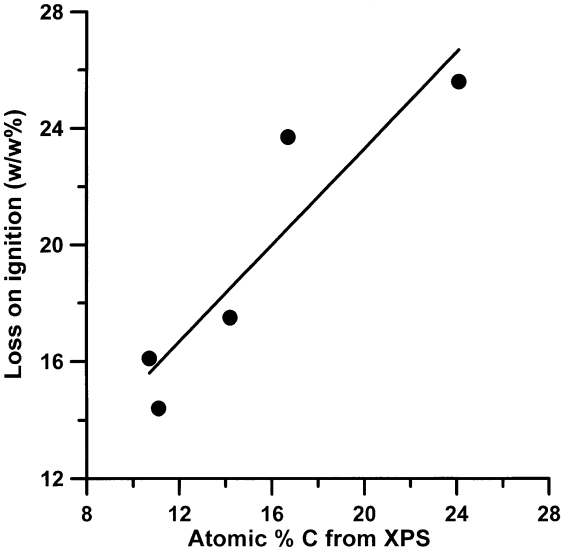

Fig. 6. Correlation between surface C and bulk organic content of finer solids.

3.7. Scanning electron microscopy

Fig. 8 shows the typical SEM micrograph of a sample of fine solids as well as the extracted coarse solids. The finer sample was found to be present as

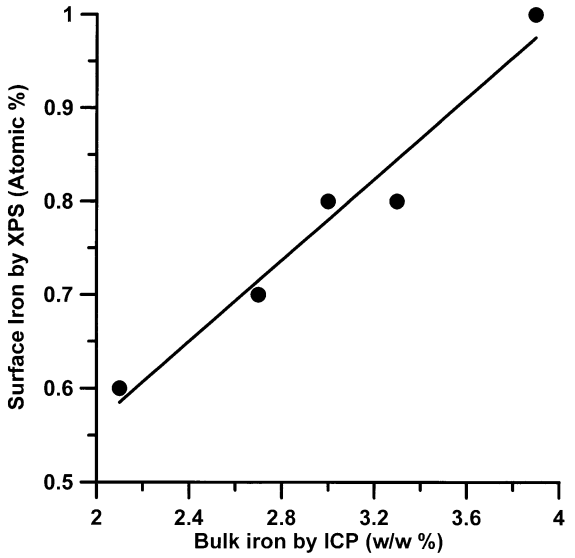

Fig. 7. Correlation between bulk and surface iron of finer solids.

agglomerates of individual particles. However, the shape and size of the individual particles showed significant variation. SEM of finer solids (Fig. 8(a)) shows planar clay flake platelets aggregated in a layered form. Large cluster of irregular plates of varying sizes and shapes is also visible in SEM photograph. The photograph also shows particles with crinkled sheet morphology.

Fig. 8(b) shows a typical SEM photograph of the extracted coarser solids. It shows a significant variation in the size and morphology of the particles. The particles are much bigger than the finer solids. Most of the particles have a rock-like appearance. A few aggregated particles are also visible. SEM photograph also shows a few chunks of porous organic matter with embedded mineral particles. Some aggregates of small platelets glued together are also visible.

3.8. Potential commercial applications

Based on the data discussed in this report, the finer solids removed from Syncrude fine tailings are essentially amorphous and are separated as a gel-like material. Industrially, the amorphous materials are useful for applications such as heterogeneous catalysis where small particle size,

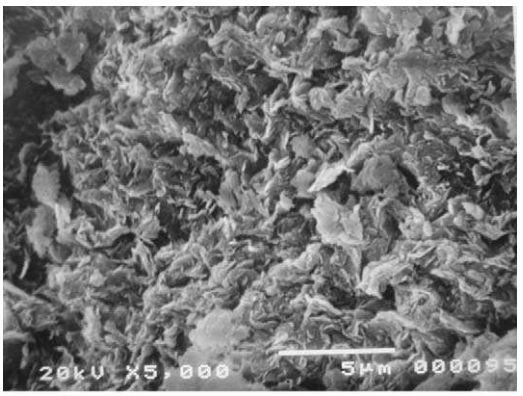

(a)

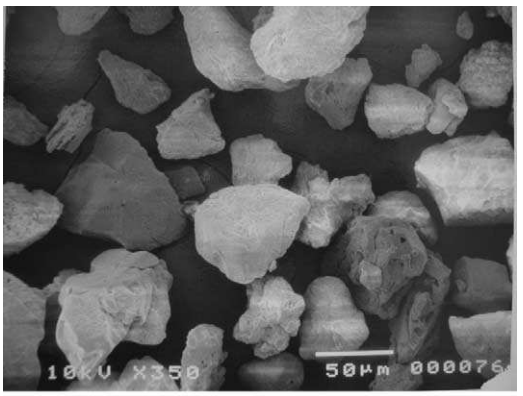

(b)

Fig. 8. A typical SEM photograph of (a) fine solids and (b) coarser solids.

high adsorption capacity, and large surface areas are important [48]. On the basis of the knowledge of structure and chemistry of the surface, it may be possible to chemically modify the surface to tailor the colloidal system to suit a particular application as sol–gel reactions provide a versatile tool for the preparation of materials with novel, designed properties. Based on the characteristics of this material, we have identified a number of commercial applications for this material. These include heterogeneous catalysis, adsorbent, conducting glass, for example, by incorporating MoS_2, microporous material, for example, for gas storage after porosity modification, for coatings, flatting (mating) agent in the paint and lacquer industry, sensor applications after encapsulating active molecules

such as dyes, enzymes, biomolecules, and hydrophobic silica after surface modification.

4. Conclusions

A very fine fraction has been separated from Syncrude fine tailings. This material was characterized using elemental analysis, X-ray powder diffraction, XPS, SEM, infrared spectroscopy, solid-state NMR, density, and surface area measurements. Several mineral phases identified in the separated colloidal solids included muscovite, kaolinite, halloysite, quartz, gibbsite, ferrihydrite, allophane, and amorphous silica. These mineral phases are associated with organic matter, either transported to the sedimentary basin or produced in situ. The poorly ordered component of fine solids such as allophanes, silica, and iron oxides may be present primarily as coatings on the surface of the well-crystallized clay particles in the fine tailings. This material can be successfully removed by dissolving in Tiron or alkalies as well as by dispersion with a dispersing agent such as sodium silicate.

The fine material separated from Syncrude fine tailings was amorphous and is characterized by large surface area, smaller particle size (20–200 nm), high absorption capacity, and large CEC. The specific surface area of this poorly ordered material was comparable with the values reported for silica–alumina gels. Surface area and pore size determine the accessibility to active sites and this is often related to catalytic activity and selectivity in catalyzed reactions. High surface area, relatively low cost, and micropores coupled with high CEC values render these materials as excellent candidates for potential applications in heterogeneous catalysis. The specific surface area of the solids was found to increase with a decrease in the amount of iron content. This suggests the agglomeration of finer particles by iron oxides thus supporting the theory of the cementation of clay particles by amorphous oxides.

Other than heterogeneous catalysis, a number of potential commercial applications have been identified for these solids. These include adsorbent, conducting glass, for example, by incorporating MoS_2, microporous material, for example, for gas storage after porosity modification, for coatings, flatting (mating) agent in the paint and lacquer industry, sensor applications after encapsulating active molecules such as dyes, enzymes, biomolecules, and hydrophobic silica after surface modification.

References

[1] F.W. Camp, The Tar Sands of Alberta, Canada, Cameron Engineering, Inc, Denver, 1969.
[2] R.N. Yong, A.J. Sethi, J. Can. Pet. Technol. 76 (1978) 76.
[3] F.W. Camp, Can. J. Chem. Eng. 55 (1977) 581.
[4] M.A. Kessick, Int. J. Miner. Process. 6 (1980) 277.
[5] B.D. Sparks, L.S. Kotlyar, A. Majid, Petroleum Society of CIM and AOSTRA Meeting, 1991, Pre-Print No. 91-117.
[6] B.D. Sparks, L.S. Kotlyar, R. Schutte, Adv. Oil Sands Tailings Research, Alberta Energy, Oil Sands Research Division, Vol. 1, 1995, p. 25.
[7] A. Majid, B.D. Sparks, Fuel 75 (1996) 879.
[8] A. Majid, J.A. Ripmeester, J. Separation Process Technol. 4 (1983) 20.
[9] A. Majid, J.A. Ripmeester, Fuel 65 (1986) 1714.
[10] A. Majid, V.P. Clancy, B.D. Sparks, Energy Fuel 2 (1988) 651.
[11] A. Majid, J. Bornais, R.A. Hutchison, Fuel Sci. Technol. Int. 7 (5–6) (1989) 507.
[12] B.D. Sparks, C.E. Capes, J.D. Hazlett, A. Majid, in: Proceedings of the International Symposium on Tailings and Effluent Management, Halifax, August 20–24, Pergamon Press, Toronto, 1989, p. 295.
[13] A. Majid, J.A. Ripmeeter, Fuel 69 (1990) 1527.
[14] A. Majid, B.D. Sparks, J. Can. Pet. Technol. 38 (11) (1999) 29.
[15] A. Majid, S. Argue, I. Kargina, V. Boyko, G. Pleizier, J. Tunney, in: Proceedings on Nanoporous Materials III, Ottawa, 2002.
[16] K. Wada, D.J. Greenland, Clay Miner. 8 (1970) 241.
[17] R.L. Downs, M.A. Ebner, W.J. Miller, in: L.C. Klein (Ed.), Sol–Gel Technology for Thin Films, Fibers, Preforms, Electronics, and Specialty Shapes, Noyes Publications, 1988.
[18] W.H. Hendershot, M. Duquette, Soil Sci. Soc. Am. J. 50 (1986) 605.
[19] M.J. Wilson, Clay Mineralogy: Spectroscopic and Chemical Determinative Methods, Chapman & Hall, London, 1994.
[20] A. Majid, B.D. Sparks, J.A. Ripmeester, Fuel 69 (1990) 145.
[21] A. Majid, B.D. Sparks, J.A. Ripmeester, Fuel 70 (1991) 78.
[22] T.S. Arnarson, R.G. Keil, Org. Geochem. 32 (2001) 1401.
[23] A. Majid, B.D. Sparks, Fuel 62 (1983) 772.
[24] S. Wada, K. Wada, Clay Miner. 12 (1977) 289.

[25] L.S.W. Sing, D.H. Everett, R.A.W. Haul, L. Moscou, R.A. Pierotti, J. Rouquerol, T. Siemieniewska, Pure Appl. Chem. 57 (1985) 603.
[26] E. Tombacz, M. Szekeres, L. Baranyi, E. Micheli, Colloid. Surf. A 141 (1998) 379.
[27] W.F. Maier, F.M. Bohnen, J. Heilmann, S. Klein, H.C. Ko, M.F. Mark, S. Thorimbert, I.C. Tilgner, M. Wiedorn, Applications of Organometallic Chemistry in the Preparation and Processing of Advanced Materials, Kluwer Academic Publishers, Boston, USA, 1995, p. 27.
[28] R.E. Grim, Clay Mineralogy, McGraw-Hill, New York, 1968.
[29] G. Zhang, K. Wasyliuk, Y. Pan, Can. Mineral. 39 (2001) 1347.
[30] T. Henmi, K. Wada, Am. Mineral. 61 (1976) 379.
[31] J.B. Dixon, S.B. Weed, Minerals in soil environment, Soil Sci. Soc. Am. (1977) 948
[32] A.S. Campbell, U. Schwertmann, Clay Miner. 20 (1985) 515.
[33] C.W. Childs, M. Matsue, N. Yoshinaga, Soil Sci. Plant Nutr. 37 (2) (1991) 299.
[34] H. Kodama, G.J. Ross, Soil Sci. Soc. Am. J. 55 (1991) 1180.
[35] G. Brown, The X-ray Identification and Crystal Structures of Clay Minerals, Mineralogical Society, London, 1961.
[36] G. Engelhardt, D. Michel, High-resolution Solid-state NMR of Silicates and Zeolites, Wiley, New York, 1987.
[37] B.A. Goodman, J.D. Russel, B. Montez, E. Oldfield, R.J. Kirkpatrick, Phys. Chem. Miner. 12 (1985) 342.
[38] L.E. DeMumbrum, Soil Sci. Soc. Am. 24 (1960) 185.
[39] L.E. DeMumbrum, Proc. Soil Sci. Soc. Am. 28 (1964) 355.
[40] J. Bertaux, F. Frohlich, P.I. ldefonse, J. Sediment Res. 68 (1998) 440.
[41] H.W. van der Marel, H. Beutelspacher, Atlas of Infrared Spectroscopy of Clay Minerals and their Admixtures, Elsevier, Amsterdam, 1976.
[42] L.J. Bellamy, The Infrared Spectra of Complex Organic Molecules, Wiley, New York, 1966.
[43] H.W. Van der Marel, P. Krohmer, Contrib. Mineral. Petrol. 22 (1969) 73.
[44] H. Van Olphen, J.J. Fripiat, Data Handbook for Clay Minerals and Other Non-metallic Minerals, Pergamon Press, New York, 1979.
[45] H. Kodama, Infrared spectra of minerals, Reference guide to identification and characterization of minerals in the study of soil, Technical Bulletin 1985-1E, Research Branch, Agricultural Canada, Ottawa, 1985.
[46] H.H.W. Moenke, in: V.C. Farmer (Ed.), The Infrared Spectra of Minerals, vol. 4, Minerlogical Society, London, 1974, p. 365 (Monograph).
[47] D.T. Harvey, R.W. Linton, Anal. Chem. 53 (1981) 1684.
[48] T.L. Barr, S. Seal, H. He, J. Klinowski, Vacuum 46 (1995) 1391.